

Study of semileptonic decays of B mesons to charmed baryons

G. Bonvicini,¹ D. Cinabro,¹ R. Greene,¹ L. P. Perera,¹ G. J. Zhou,¹ M. Chadha,² S. Chan,² G. Eigen,² J. S. Miller,² C. O'Grady,² M. Schmidtler,² J. Urheim,² A. J. Weinstein,² F. Würthwein,² D. W. Bliss,³ G. Masek,³ H. P. Paar,³ S. Prell,³ V. Sharma,³ D. M. Asner,⁴ J. Gronberg,⁴ T. S. Hill,⁴ D. J. Lange,⁴ R. J. Morrison,⁴ H. N. Nelson,⁴ T. K. Nelson,⁴ D. Roberts,⁴ A. Ryd,⁴ R. Balest,⁵ B. H. Behrens,⁵ W. T. Ford,⁵ H. Park,⁵ J. Roy,⁵ J. G. Smith,⁵ J. P. Alexander,⁶ R. Baker,⁶ C. Bebek,⁶ B. E. Berger,⁶ K. Berkelman,⁶ K. Bloom,⁶ V. Boisvert,⁶ D. G. Cassel,⁶ D. S. Crowcroft,⁶ M. Dickson,⁶ S. von Dombrowski,⁶ P. S. Drell,⁶ K. M. Ecklund,⁶ R. Ehrlich,⁶ A. D. Foland,⁶ P. Gaidarev,⁶ L. Gibbons,⁶ B. Gittelman,⁶ S. W. Gray,⁶ D. L. Hartill,⁶ B. K. Heltsley,⁶ P. I. Hopman,⁶ J. Kandaswamy,⁶ P. C. Kim,⁶ D. L. Kreinick,⁶ T. Lee,⁶ Y. Liu,⁶ N. B. Mistry,⁶ C. R. Ng,⁶ E. Nordberg,⁶ M. Ogg,^{6,*} J. R. Patterson,⁶ D. Peterson,⁶ D. Riley,⁶ A. Soffer,⁶ B. Valant-Spaight,⁶ C. Ward,⁶ M. Athanas,⁷ P. Avery,⁷ C. D. Jones,⁷ M. Lohner,⁷ S. Patton,⁷ C. Prescott,⁷ J. Yelton,⁷ J. Zheng,⁷ G. Brandenburg,⁸ R. A. Briere,⁸ A. Ershov,⁸ Y. S. Gao,⁸ D. Y.-J. Kim,⁸ R. Wilson,⁸ H. Yamamoto,⁸ T. E. Browder,⁹ Y. Li,⁹ J. L. Rodriguez,⁹ T. Bergfeld,¹⁰ B. I. Eisenstein,¹⁰ J. Ernst,¹⁰ G. E. Gladding,¹⁰ G. D. Gollin,¹⁰ R. M. Hans,¹⁰ E. Johnson,¹⁰ I. Karliner,¹⁰ M. A. Marsh,¹⁰ M. Palmer,¹⁰ M. Selen,¹⁰ J. J. Thaler,¹⁰ K. W. Edwards,¹¹ A. Bellerive,¹² R. Janicek,¹² D. B. MacFarlane,¹² P. M. Patel,¹² A. J. Sadoff,¹³ R. Ammar,¹⁴ P. Baringer,¹⁴ A. Bean,¹⁴ D. Besson,¹⁴ D. Coppage,¹⁴ C. Darling,¹⁴ R. Davis,¹⁴ S. Kotov,¹⁴ I. Kravchenko,¹⁴ N. Kwak,¹⁴ L. Zhou,¹⁴ S. Anderson,¹⁵ Y. Kubota,¹⁵ S. J. Lee,¹⁵ J. J. O'Neill,¹⁵ R. Poling,¹⁵ T. Riehle,¹⁵ A. Smith,¹⁵ M. S. Alam,¹⁶ S. B. Athar,¹⁶ Z. Ling,¹⁶ A. H. Mahmood,¹⁶ S. Timm,¹⁶ F. Wappler,¹⁶ A. Anastassov,¹⁷ J. E. Duboscq,¹⁷ D. Fujino,^{17,†} K. K. Gan,¹⁷ T. Hart,¹⁷ K. Honscheid,¹⁷ H. Kagan,¹⁷ R. Kass,¹⁷ J. Lee,¹⁷ M. B. Spencer,¹⁷ M. Sung,¹⁷ A. Undrus,^{17,‡} R. Wanke,¹⁷ A. Wolf,¹⁷ M. M. Zoeller,¹⁷ B. Nemati,¹⁸ S. J. Richichi,¹⁸ W. R. Ross,¹⁸ H. Severini,¹⁸ P. Skubic,¹⁸ M. Bishai,¹⁹ J. Fast,¹⁹ J. W. Hinson,¹⁹ N. Menon,¹⁹ D. H. Miller,¹⁹ E. I. Shibata,¹⁹ I. P. J. Shipsey,¹⁹ M. Yurko,¹⁹ S. Glenn,²⁰ S. D. Johnson,²⁰ Y. Kwon,^{20,§} S. Roberts,²⁰ E. H. Thorndike,²⁰ C. P. Jessop,²¹ K. Lingel,²¹ H. Marsiske,²¹ M. L. Perl,²¹ V. Savinov,²¹ D. Ugolini,²¹ R. Wang,²¹ X. Zhou,²¹ T. E. Coan,²² V. Fadeyev,²² I. Korolkov,²² Y. Maravin,²² I. Narsky,²² V. Shelkov,²² J. Staeck,²² R. Stroynowski,²² I. Volobouev,²² J. Ye,²² M. Artuso,²³ F. Azfar,²³ A. Efimov,²³ M. Goldberg,²³ D. He,²³ S. Kopp,²³ G. C. Moneti,²³ R. Mountain,²³ S. Schuh,²³ T. Skwarnicki,²³ S. Stone,²³ G. Viehhauser,²³ X. Xing,²³ J. Bartelt,²⁴ S. E. Csorna,²⁴ V. Jain,^{24,||} K. W. McLean,²⁴ S. Marka,²⁴ R. Godang,²⁵ K. Kinoshita,²⁵ I. C. Lai,²⁵ P. Pomianowski,²⁵ and S. Schrenk²⁵

(CLEO Collaboration)

¹Wayne State University, Detroit, Michigan 48202²California Institute of Technology, Pasadena, California 91125³University of California, San Diego, La Jolla, California 92093⁴University of California, Santa Barbara, California 93106⁵University of Colorado, Boulder, Colorado 80309-0390⁶Cornell University, Ithaca, New York 14853⁷University of Florida, Gainesville, Florida 32611⁸Harvard University, Cambridge, Massachusetts 02138⁹University of Hawaii at Manoa, Honolulu, Hawaii 96822¹⁰University of Illinois, Urbana-Champaign, Illinois 61801¹¹Carleton University, Ottawa, Ontario, Canada K1S 5B6

and the Institute of Particle Physics, Canada

¹²McGill University, Montréal, Québec, Canada H3A 2T8

and the Institute of Particle Physics, Canada

¹³Ithaca College, Ithaca, New York 14850¹⁴University of Kansas, Lawrence, Kansas 66045¹⁵University of Minnesota, Minneapolis, Minnesota 55455¹⁶State University of New York at Albany, Albany, New York 12222¹⁷Ohio State University, Columbus, Ohio 43210¹⁸University of Oklahoma, Norman, Oklahoma 73019¹⁹Purdue University, West Lafayette, Indiana 47907²⁰University of Rochester, Rochester, New York 14627²¹Stanford Linear Accelerator Center, Stanford University, Stanford, California 94309²²Southern Methodist University, Dallas, Texas 75275²³Syracuse University, Syracuse, New York 13244²⁴Vanderbilt University, Nashville, Tennessee 37235²⁵Virginia Polytechnic Institute and State University, Blacksburg, Virginia 24061

(Received 2 December 1997; published 14 April 1998)

Using data collected by the CLEO II detector at a center-of-mass energy on or near the $Y(4S)$ resonance, we have determined the 90% confidence level upper limit $\mathcal{B}(\bar{B} \rightarrow \Lambda_c^+ e^- X) / \mathcal{B}(\bar{B} \rightarrow (\Lambda_c^+ \text{ or } \bar{\Lambda}_c^-) X) < 0.05$ for electrons with momentum above 0.6 GeV/ c . We have also obtained the limit $\mathcal{B}(B^- \rightarrow \Lambda_c^+ \bar{p} e^- \bar{\nu}_e) / \mathcal{B}(\bar{B} \rightarrow \Lambda_c^+ \bar{p} X) < 0.04$ at the 90% confidence level and measured the ratio $\mathcal{B}(\bar{B} \rightarrow \Lambda_c^+ \bar{p} X) / \mathcal{B}(\bar{B} \rightarrow (\Lambda_c^+ \text{ or } \bar{\Lambda}_c^-) X) = 0.57 \pm 0.05 \pm 0.05$. [S0556-2821(98)03111-7]

PACS number(s): 13.20.He

I. INTRODUCTION

In the naive spectator model, most B mesons decay through the spectator diagram with semileptonic decays occurring by ‘‘external’’ W -emission: $b \rightarrow cW$; $W \rightarrow \ell \bar{\nu}_\ell$. In this picture, charmed baryon production occurs when two quark-antiquark pairs from the vacuum bind with the charm quark and the spectator antiquark to form a $\Lambda_c^+(cud)$ plus an antinucleon \bar{N} . In this paper we attempt to isolate the magnitude of this external W -emission spectator diagram in charmed baryon decays by measuring $\bar{B} \rightarrow \Lambda_c^+ e^- X$ and $B^- \rightarrow \Lambda_c^+ \bar{p} e^- \bar{\nu}_e$. For normalization modes, we also measure $\bar{B} \rightarrow \Lambda_c^+ \bar{p} X$ and $\bar{B} \rightarrow (\Lambda_c^+ \text{ or } \bar{\Lambda}_c^-) X$. Throughout this paper charged conjugate modes are implicit.

If $B \rightarrow$ baryons does indeed occur through external W -emission as outlined above, then the decay $\bar{B} \rightarrow \Lambda_c^+ \bar{N} X e^- \bar{\nu}_\ell$ will occur [1]. We can estimate the magnitude of $R = \mathcal{B}(\bar{B} \rightarrow \Lambda_c^+ \bar{N} e^- \bar{\nu}_\ell) / \mathcal{B}(\bar{B} \rightarrow \Lambda_c^+ \bar{N} X)$ by using the naive expectation for the semileptonic branching ratio in these decays. The $(\bar{c}s)$ and $(\tau \bar{\nu}_\tau)$ contributions are absent due to the limited available phase space, and so a maximum of 20% is expected for the ratio R . Alternately, one might anticipate that $\mathcal{B}(\bar{B} \rightarrow \Lambda_c^+ X e^- \bar{\nu}_e) / \mathcal{B}(\bar{B} \rightarrow \Lambda_c^+ X)$ is comparable to the measurements of $\mathcal{B}(\bar{B} \rightarrow D X e^- \bar{\nu}_e) / \mathcal{B}(\bar{B} \rightarrow D X) \approx 12\%$ [2].

There are two other baryon production mechanisms in B decay, neither making a contribution to semileptonic decay. In one, the W is emitted internally and decays to $(\bar{c}s)$, leading to $\Xi_c \bar{\Lambda}_c$ final states. This mechanism was studied in a previous CLEO paper, which looked at the charge correlations between Λ_c 's and leptons from B decay and found $R_{\Lambda_c} = N_{\bar{\Lambda}_c^- \ell^+} / N_{\Lambda_c^+ \ell^+} = \mathcal{B}(\bar{B} \rightarrow \bar{\Lambda}_c^- X) \mathcal{B}(B \rightarrow X \ell^+ \nu_\ell) / \mathcal{B}(\bar{B} \rightarrow \Lambda_c^+ X) \mathcal{B}(B \rightarrow X \ell^+ \nu_\ell) = 0.19 \pm 0.13 \pm 0.04$ which is directly related to $\mathcal{B}(b \rightarrow c \bar{c} s) / \mathcal{B}(b \rightarrow c \bar{u} d)$ [3]. For $\Lambda_c X$ final states, we cannot rule out the possibility in our analysis that we are observing decays of the type $\bar{B} \rightarrow \Xi_c \bar{\Lambda}_c$, as we cannot tag the parent B meson in the $\bar{B} \rightarrow \Lambda_c^+ X$ analysis. Therefore, the yields for this mode will be quoted as decays of the type $\bar{B} \rightarrow (\Lambda_c^+ \text{ or } \bar{\Lambda}_c^-) X$. Another mechanism is the

internal emission of a W followed by its decay to $(\bar{u}d)$. Measurements of B mesons decaying hadronically to charmed baryons indicate that this internal W -emission diagram may contribute significantly [4]. A substantial contribution from this diagram would reduce the semileptonic decay width.

The semileptonic branching ratio of B mesons is known to have a lower value than theoretical predictions [5]. These predictions assume a large external W -emission contribution in baryon decays. The suggestion has been made that theory may underestimate the B -hadronic width by neglecting B decay channels to baryon states [6]. If this is the case, hadronic decays to charmed baryons could explain the low inclusive semileptonic branching ratio. The measurement of semileptonic decays of B mesons to Λ_c will provide vital information on baryon production in B decays.

A. Data sample and event selection

The data were taken with the CLEO II detector [7] at the Cornell Electron Storage Ring (CESR), and consist of 3.2 fb^{-1} on the $Y(4S)$ resonance and 1.6 fb^{-1} at a center-of-mass energy 60 MeV below the resonance. The on-resonance sample contains 3.4×10^6 $B\bar{B}$ events and 10×10^6 continuum events. We select hadronic events containing at least 4 charged tracks. To suppress continuum background, we require the ratio of Fox-Wolfram moments [8] $R_2 = H_2 / H_0$ to satisfy $R_2 \leq 0.35$. We reconstruct Λ_c 's in the $pK\pi$ decay mode. For the hadronic particle identification, a probability cut for each target hadron is made which uses information obtained from dE/dx and time-of-flight detectors. For particle consistency, the probability cuts are chosen to be greater than 0.0027 (within three standard deviations of the expected value) for pions, 0.0001 for kaons, and 0.0003 for protons. Continuum data are used to directly subtract backgrounds from non- $B\bar{B}$ events.

Tagged signal Monte Carlo simulated events were used to obtain the signal efficiencies while $B\bar{B}$ Monte Carlo simulated events, with the signal channel removed, were used to estimate the background from B decays to non-signal modes. The CLEO $B\bar{B}$ Monte Carlo simulation generates baryonic decays with a phenomenological model which is tuned to match the observed Λ_c momentum spectrum. We use $B\bar{B}$ Monte Carlo events where we force the $\bar{B} \rightarrow \Lambda_c^+ X$, $\Lambda_c^+ \rightarrow pK^- \pi^+$ decay chain to determine a detection efficiency of 0.36 ± 0.01 .

The $pK^- \pi^+$ invariant mass distributions are measured separately for the resonance and continuum data. The resonance data are fitted to a double Gaussian signal atop a low-order polynomial background. In these fits, the width of the Gaussian Λ_c signal function is constrained to the value de-

*Permanent address: University of Texas, Austin TX 78712.

†Permanent address: Lawrence Livermore National Laboratory, Livermore, CA 94551.

‡Permanent address: BINP, RU-630090 Novosibirsk, Russia.

§Permanent address: Yonsei University, Seoul 120-749, Korea.

||Permanent address: Brookhaven National Laboratory, Upton, NY 11973.

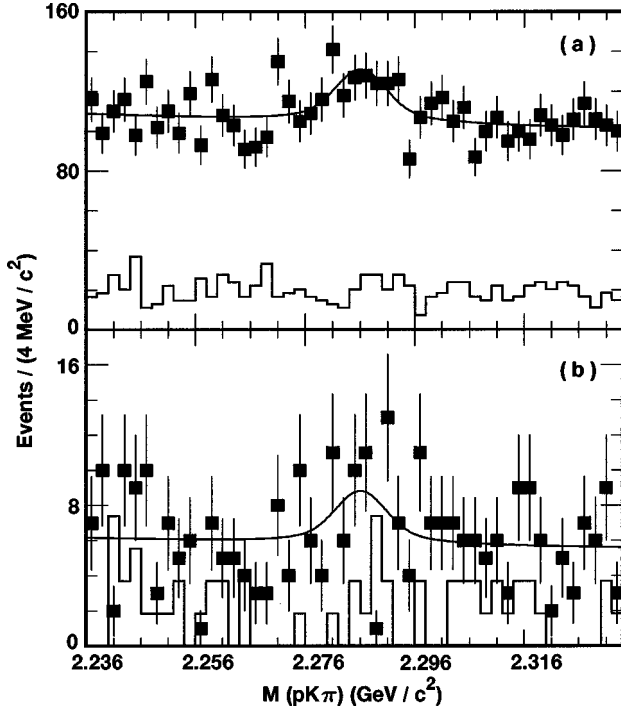


FIG. 1. The fit (line) to the $pK^- \pi^+$ invariant mass spectrum from on resonance data events (points with error bars) and the scaled off resonance data (histogram) for the (a) $\bar{B} \rightarrow \Lambda_c^+ e^- X$ and (b) $B^- \rightarrow \Lambda_c^+ p e^- \bar{\nu}_e$ analyses.

rived from the Monte Carlo simulation. After subtracting non- $B\bar{B}$ contributions using off-resonance data scaled for luminosity and cross section, we obtain a total sample of $4879 \pm 296 \bar{B} \rightarrow (\Lambda_c^+ \text{ or } \bar{\Lambda}_c^-) X$ events from data. After scaling by the efficiency, we find a yield of $13552 \pm 822 \pm 802$ events, where the second (systematic) error includes contributions from the efficiency correction.

B. Study of $\bar{B} \rightarrow \Lambda_c^+ e^- X$

Because of the soft lepton momentum spectrum from this decay and the limited reconstruction efficiency for low momentum muons, we use only electrons in our analysis. Electron identification relies on E/p measurements derived from the calorimeter and drift chamber, as well as specific ionization loss measurements from the drift chamber. The requirement of $\ln(P_e/P_\ell) > 3.0$ is imposed, where $P_e(P_\ell)$ is the

probability that a given charged track is an electron (not an electron). We choose a minimum momentum cutoff of $0.6 \text{ GeV}/c$ for these electrons to limit fake and secondary electron background sources. The maximum possible electron momentum for this decay is $1.5 \text{ GeV}/c$. Electron candidates are restricted to the polar angular region $|\cos \theta| \leq 0.71$. We pair all $pK^- \pi^+$ candidates, selected as described above, with additional tracks in the events passing the lepton identification requirement. We then fit the $pK^- \pi^+$ invariant mass distributions on and off resonance for combinations passing these cuts.

Figure 1(a) shows the fit to the $pK^- \pi^+$ invariant mass distribution for events that satisfy the above selection criteria. The resonance data (points) are fit to a double Gaussian signal over a second order polynomial background. The signal shape is fixed to that from the data in the $\bar{B} \rightarrow \Lambda_c^+ X$ analysis. A similar fit has been performed on the $pK^- \pi^+$ invariant mass distribution from the continuum data (shown by the scaled histogram in the figure). The yields are given in Table I.

In addition to continuum Λ_c^+ 's, other sources of background are fake leptons and uncorrelated $\Lambda_c^+ - e^-$ pairs. The number of fake leptons is obtained by running the same analysis, but using an electron anti-identification criterion: $\ln(P_e/P_\ell) < 0$. The $pK^- \pi^+$ invariant mass is refit and this yield is scaled by the measured lepton misidentification probabilities. The uncorrelated background includes combinations where the Λ_c^+ originates from \bar{B} decay and the lepton originates from B decay or from a \bar{B} if from an event where mixing took place. This background is estimated using $\bar{B} \rightarrow \Lambda_c^+ X$ Monte Carlo events and examining decays where the Λ_c^+ and e^- have opposite charges, but do not originate from the signal mode. We check this procedure by comparing the data and Monte Carlo results obtained using $\Lambda_c^+ e^+$ (wrong sign) combinations. Wrong sign combinations will include primary leptons from one B paired with Λ_c^+ 's from the other B . We find consistency between the data and Monte Carlo wrong sign yields. The background predictions are given in Table I.

The lepton minimum momentum cut of $0.6 \text{ GeV}/c$ results in a model dependence. Larger multiplicity final states will have a lower efficiency due to the minimum momentum cut. We find the efficiency using $B^- \rightarrow \Lambda_c^+ p e^- \bar{\nu}_e$ Monte Carlo events where the B^+ decays generically. This efficiency for

TABLE I. Results of the $\Lambda_c^+ e^- X$, $\Lambda_c^+ p e^- \bar{\nu}_e$, and $\Lambda_c^+ p X$ analyses. The ‘‘Data on’’ row shows results from fits to the on resonance data sample, while the ‘‘Scaled off’’ row shows the results of the fits to the nearby continuum data scaled for luminosity and cross section.

Type	$\Lambda_c^+ e^- X$	$\Lambda_c^+ p e^- \bar{\nu}_e$	$\Lambda_c^+ p X$
Data on	176 ± 41	20 ± 10	2501 ± 121
Scaled off	9 ± 22	6 ± 7	440 ± 105
Fakes	10 ± 4 (e)	2 ± 1 (e and \bar{p})	$32_{-15}^{+6}(\bar{p}^+ s)$
MC pred. uncorr.	$95 \pm 7 \pm 33$	11 ± 6	$58 \pm 6 \pm 58$
Bkgd. sub.	$62 \pm 47 \pm 34$	$1 \pm 12 \pm 6$	$1971 \pm 160_{-60}^{+59}$
Efficiencies	$0.239 \pm 0.005 \pm 0.011$	$0.094 \pm 0.003 \pm 0.003$	$0.257 \pm 0.003 \pm 0.010$
Yield	$259 \pm 196 \pm 143$	$11 \pm 132 \pm 82$	$7669 \pm 623 \pm 385$

$B^- \rightarrow \Lambda_c^+ \bar{p} e^- \bar{\nu}_e$, where the electron is prompt from the B decay, is found to be 17%. Monte Carlo events from the chain $\bar{B}^0 \rightarrow \Lambda_c^+ \bar{\Delta}^0 e^- \bar{\nu}_e$, $\bar{\Delta}^0 \rightarrow \bar{p} \pi^+$ were also generated to measure the efficiency. This mode adds one extra pion to the total decay chain although more could be present in other decays such as $\bar{B} \rightarrow \Sigma_c \bar{\Delta} e \nu$. Differences between efficiencies for B^- and \bar{B}^0 are found to be negligible. After all other cuts, we find that 73% of the events from $B^- \rightarrow \Lambda_c^+ \bar{p} e^- \bar{\nu}_e$ pass our electron momentum cut while only 45% of the events from $\bar{B}^0 \rightarrow \Lambda_c^+ \bar{\Delta}^0 e^- \bar{\nu}_e$ pass. Because the total efficiency is dependent on the number of pions in the final state, we choose to quote a partial branching fraction where the lepton momentum is greater than $0.6 \text{ GeV}/c$. In this electron momentum range, the efficiency for $\bar{B} \rightarrow \Lambda_c^+ \bar{p} e^- \bar{\nu}_e$ is 0.239 ± 0.005 which is consistent with the efficiency for other modes with extra pions. In addition to assigning a systematic error due to efficiency determination, we add in quadrature errors from the fake lepton and uncorrelated background source estimates to obtain the total systematic error.

C. Search for $B^- \rightarrow \Lambda_c^+ \bar{p} e^- \bar{\nu}_e$

The signature of $B^- \rightarrow \Lambda_c^+ \bar{p} e^- \bar{\nu}_e$ is a baryon-lepton-antiproton combination which has a recoil mass consistent with that of a neutrino, approximating the B momentum as zero. Candidate Λ_c^+ 's, electrons, and antiprotons for the analysis must satisfy requirements similar to those discussed above. We then require that the approximation of the squared mass of the neutrino, $\bar{M}_\nu^2 \equiv (E_{\text{beam}} - E_{\Lambda_c} - E_e)^2 - (\mathbf{p}_{\Lambda_c} + \mathbf{p}_e)^2$, be greater than $-2(\text{GeV}/c^2)^2$. In addition, we place an angular cut of $\cos \theta_{\Lambda_c e} < -0.2$, where $\theta_{\Lambda_c e}$ is the angle between the Λ_c^+ and electron. In Fig. 1(b) we show the Λ_c^+ invariant mass distribution for combinations passing all of these cuts. This distribution is fit as before; results are given in Table I.

Backgrounds to this process stem from three sources: fake antiprotons or electrons, non- $B\bar{B}$ events, and secondary electrons or antiprotons. Fake antiprotons and electrons are considered separately. We use the same methods as described above to determine each contribution. The continuum background is measured using the off-resonance data scaled for luminosity and cross section. The remaining background events, in which electrons come from the decay chain $\bar{b} \rightarrow \bar{c} \rightarrow \bar{s} e \nu$, can be estimated using a Monte Carlo simulation. The wrong sign data and Monte Carlo results are compared and again found to agree well.

We find efficiency using the $B^- \rightarrow \Lambda_c^+ \bar{p} e^- \bar{\nu}_e$ Monte Carlo events where the B^+ decays generically. The efficiency is found to be 0.094 ± 0.003 . Systematic errors are assigned for each of the background source estimates and the efficiency determination as described above.

D. Study of $\bar{B} \rightarrow \Lambda_c^+ \bar{p} X$

We pair all Λ_c^+ and \bar{p} candidates using the Λ_c^+ selection as described above. For the \bar{p} , in addition to the cut on the proton probability of greater than 0.0003, we employ addi-

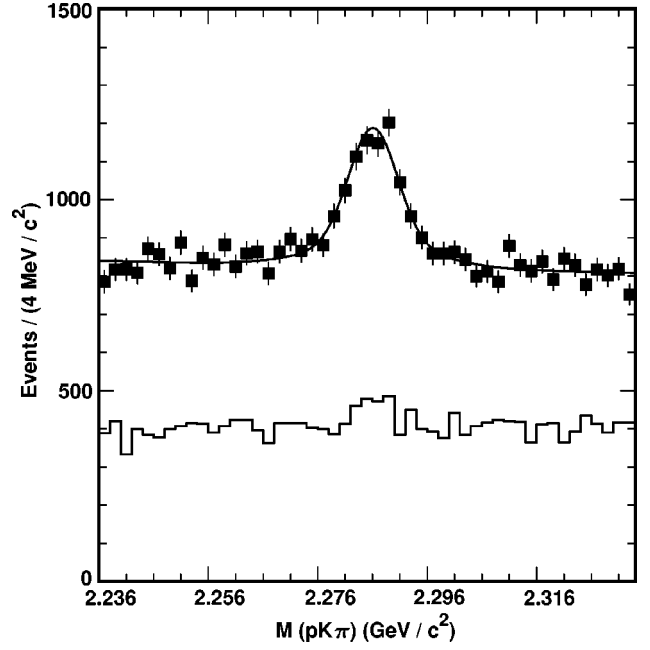


FIG. 2. The fit (line) to the $pK^- \pi^+$ invariant mass spectrum from on resonance data events (points with error bars) and the scaled off resonance data (histogram) for the $\bar{B} \rightarrow \Lambda_c^+ \bar{p} X$ analysis.

tional veto cuts on the particle identification of 2σ for the π , K , and electron to reduce fake antiprotons. We then fit the Λ_c^+ invariant mass. The observed Λ_c^+ signal area then measures the number of $\Lambda_c^+ - \bar{p}$ correlations. Figure 2 shows the fit to the data.

We are looking for decays where the Λ_c^+ and \bar{p} have opposite charge and both are primary from the B decay. Backgrounds are categorized into two sources: secondary \bar{p} (not primary from a B decay) and fake \bar{p} . The first background source is estimated by using $\bar{B} \rightarrow \Lambda_c^+ X$ Monte Carlo events as above. Once again we check this procedure by comparing wrong sign data yields to our Monte Carlo wrong sign prediction. Proton misidentification probabilities are also measured directly from the data by using a pion sample from $K_S^0 \rightarrow \pi^+ \pi^-$ where K_S^0 's are selected by a secondary vertex finder. After applying the veto cuts for kaons, pions, and electrons, the fake probability derived from just using the pion rate is found to be consistent with the species averaged rate. The background contribution of fake \bar{p} 's is obtained by running the same analysis without the particle identification cuts for the \bar{p} correlated with Λ_c^+ . The yields obtained from fits to the $pK^- \pi^+$ mass are then multiplied by the faking \bar{p} probabilities and weighted by momentum. This procedure will yield an upper limit on the number of fakes, as real proton tracks are double counted in our procedure. We studied the overcounting rate and assign a systematic error based on the difference between the number of protons counted with no identification criteria and the number counted using the anti-identification criteria.

We have also measured the absolute proton identification efficiency as a function of momentum for the cuts in this analysis using a sample of $\Lambda \rightarrow p \pi^-$ events. The differences in the identification efficiencies between the data and Monte Carlo prediction are then used to calculate the systematic

error in the $\mathcal{B}(\bar{B} \rightarrow \Lambda_c^+ \bar{p} X) / \mathcal{B}(\bar{B} \rightarrow \Lambda_c^+ X)$ measurement (Table I). The total systematic error for this mode is then derived from errors in the efficiency as well as background determinations.

II. SUMMARY

Table I summarizes the final numbers of candidates for the three signal modes. After background subtraction, the number of wrong sign candidates observed in the data is consistent with our expectations based on Monte Carlo studies.

We measure the ratio

$$\frac{\mathcal{B}(\bar{B} \rightarrow \Lambda_c^+ \bar{p} X)}{\mathcal{B}(\bar{B} \rightarrow (\Lambda_c^+ \text{ or } \bar{\Lambda}_c^-) X)} = \frac{(7669 \pm 623 \pm 385)}{(13552 \pm 822 \pm 802)} = 0.57 \pm 0.05 \pm 0.05, \quad (1)$$

consistent with the naively expected value of 50%.

For the electron channels, the number of signal candidates is fully consistent with the expected background level, and so we derive a 90% confidence level upper limit for the ratio R , for $p_e \geq 0.6$ GeV/ c :

$$R = \frac{\mathcal{B}(\bar{B} \rightarrow \Lambda_c^+ e^- X)}{\mathcal{B}(\bar{B} \rightarrow (\Lambda_c^+ \text{ or } \bar{\Lambda}_c^-) X)} = \frac{(259 \pm 196 \pm 143)}{(13552 \pm 822 \pm 802)} < 0.05 \text{ at } 90\% \text{ C.L.} \quad (2)$$

If one assumes that all of the semileptonic decays proceed via the channel $B^- \rightarrow \Lambda_c^+ \bar{p} e^- \bar{\nu}_e$, the upper limit on R would be 0.07 for the entire electron momentum range. Similarly, if all of the semileptonic decays were $\bar{B}^0 \rightarrow \Lambda_c^+ \bar{\Delta}^0 e^- \bar{\nu}_e$, the limit on R would be 0.11. Our result is consistent with the derived limit based on a previous measurement where the charmed baryon is not observed and the lepton spectrum is

extrapolated from a model of $\mathcal{B}(\bar{B} \rightarrow X \bar{p} e^- \bar{\nu}_e) < 0.16\%$ at 90% C.L. [9]. This implies a limit on $\mathcal{B}(\bar{B} \rightarrow \Lambda_c^+ e^- X) / \mathcal{B}(\bar{B} \rightarrow (\Lambda_c^+ \text{ or } \bar{\Lambda}_c^-) X) < 5\%$ at 90% C.L.

For the $\Lambda_c \bar{p} e \bar{\nu}_e$ channel, we find

$$\frac{\mathcal{B}(B^- \rightarrow \Lambda_c^+ \bar{p} e^- \bar{\nu}_e)}{\mathcal{B}(\bar{B} \rightarrow \Lambda_c^+ \bar{p} X)} < 0.04 \text{ at } 90\% \text{ C.L.} \quad (3)$$

for the entire electron momentum range.

Our limits on the semileptonic branching ratios do not support the hypothesis that the external W -emission diagram saturates charmed baryon production in B decays. While the $\mathcal{B}(\bar{B} \rightarrow \Lambda_c^+ e^- X)$ measurement is limited by our knowledge of the possible decay states, the exclusive limit constrains the expected dominant mode below the corresponding rate measured for B decays to charmed mesons. The semileptonic decay rate from B to baryons does not add a large contribution to the total semileptonic B decay rate if these semileptonic decays are dominated by modes of the type $\bar{B} \rightarrow \Lambda_c^+ \bar{N} e^- \bar{\nu}_e$.

ACKNOWLEDGMENTS

We gratefully acknowledge the effort of the CESR staff in providing us with excellent luminosity and running conditions. J.P.A., J.R.P., and I.P.J.S. thank the NYI program of the NSF, M.S. thanks the PFF program of the NSF, G.E. thanks the Heisenberg Foundation, K.K.G., M.S., H.N.N., T.S., and H.Y. thank the OJI program of the DOE, J.R.P., K.H., M.S. and V.S. thank the A.P. Sloan Foundation, R.W. thanks the Alexander von Humboldt Stiftung, M.S. thanks Research Corporation, and S.D. thanks the Swiss National Science Foundation for support. This work was supported by the National Science Foundation, the U.S. Department of Energy, and the Natural Sciences and Engineering Research Council of Canada.

[1] G. Crawford *et al.*, Phys. Rev. D **45**, 752 (1992).
 [2] Particle Data Group, R. M. Barnett *et al.*, Phys. Rev. D **54**, 1 (1996).
 [3] R. Ammar *et al.*, Phys. Rev. D **55**, 13 (1997).
 [4] M. Procaro *et al.*, Phys. Rev. Lett. **73**, 1472 (1994).
 [5] I. Bigi *et al.*, Phys. Lett. B **323**, 408 (1994).

[6] I. Dunietz, P. Cooper, A. Falk, and M. Wise, Phys. Rev. Lett. **73**, 1075 (1994).
 [7] Y. Kubota *et al.*, Nucl. Instrum. Methods Phys. Res. A **320**, 66 (1992).
 [8] G. C. Fox and S. Wolfram, Phys. Rev. Lett. **41**, 1581 (1978).
 [9] H. Albrecht *et al.*, Phys. Lett. B **249**, 359 (1990).